Congresso de Métodos Numéricos em Engenharia 2015
Lisboa, 29 de Junho a 2 de Julho 2015

ANALYSIS AND DESIGN OF HORN ANTENNAS WITH ARBITRARY PROFILE USING MODE-MATCHING

Lucas Polo-López[1], Jorge A. Ruiz-Cruz[1], Juan Córcoles[1] and Carlos A. Leal-Sevillano[2]

1: Escuela Politécnica Superior
Universidad Autónoma de Madrid
Calle Francisco Tomás y Valiente, 11. 28049 Madrid
e-mail: lucas.polo@estudiante.uam.es, web: http://rfcas.eps.uam.es

2: ETSI Telecomunicación
Universidad Politécnica de Madrid
Avenida Complutense, 30. 28040 Madrid
e-mail: caleal@etc.upm.es, web: http://www.etsit.upm.es

Keywords:
antenna, horn, mode-matching, waveguide mode, scattering matrix, radiation pattern

Abstract.
One drawback of horn antennas is the difficulty in performing the required computations for their analysis and design. With the actual development of CAD tools these problems have been reduced but they are still far from being completely solved. Most commercial CAD tools employ general-purpose numerical techniques (like Finite Differences Method and Finite Elements Method) since they allow using the same software to simulate a wide range of devices. The disadvantage of these methods lies on the fact that this generality comes at a cost, the loss of efficiency. On the other hand, quasi-analytical techniques are usually more efficient but they can only work with a narrow spectrum of problems.

The main objective of this work is to develop a software tool capable of analysing, simulating and designing horn antennas efficiently. To accomplish this, a quasi-analytical method called Mode-Matching will be used.

1 INTRODUCTION

Horn antennas belong to the family of aperture antennas. They usually consist of a waveguide whose transverse section increases along the longitudinal dimension, allowing the wave that propagates inside the waveguide to propagate in free space. These antennas present high values of directivity and gain that, along with its physical robustness and high efficiency, make them perfect candidates for critical applications like aerospace communications [1].

The accurate analysis and design of horn antennas involves the study of the electromagnetic modes inside the horn and the computation of the radiation pattern based on the modes at the aperture of the antenna. In the past, these tasks were traditionally tackled using approximations, but these techniques usually lead to imprecise results since they do not consider some of the high frequency effects that appear when working with microwave devices.

The development of CAD tools opened the possibility of using numerical techniques instead of circuital approximations, achieving therefore more accurate results. These techniques can be classified in general-purpose and quasi-analytical. The first group includes methods like Finite Differences and Finite Elements, and most of the commercial CAD tools implement techniques that belong to this family. The main reason of doing this is because general-purpose methods can work with a large range of different problems. Of course, this advantage has an associated disadvantage and this generality often makes general-purpose methods highly inefficient, leading to large computation times. On the other hand, quasi-analytical techniques are specifically crafted to solve a narrow spectrum of problems [2] which grants them with high efficiency levels, obtaining significantly shorter computation requirements.

In this work, a software tool capable of analysing and designing horn antennas efficiently will be developed, using the approach in [3]. A very efficient home-made implementation of the Mode-Matching code [4] will be used to model the inner-part of the horn. The high computational efficiency achieved by this method will make this implementation specially suited to be combined with an optimization algorithm in order to get an automatic design tool that, given a set of specifications on the radiation characteristics, will give a description of a horn fulfilling them.

The following paper is structured into four sections, covering different aspects involved in the process of developing an analysis and design tool based on a numerical method. In section 2 the Mode-Matching method is presented and its main equations are derived. The interested reader may find the complete derivation at [4].

The details on how to apply this numerical method to model horn antennas are explained in section 3. After this, some simulation results obtained with the developed tool are shown in section 4, comparing the obtained data with measurements and simulations from different authors.

Finally, in section 5 the main advantages of the method are highlighted and some insight on how to use Mode-Matching techniques to design horn antennas is given.

2 MODE-MATCHING METHOD FOR WAVEGUIDE STEPS

In the Mode-Matching method, first of all, the problem (the device) under analysis must be segmented in regions. In each of these regions the electromagnetic fields $(\vec{\mathbf{E}}, \vec{\mathbf{H}})$ can be represented as the superposition of modes [2][4][5]:

$$\vec{\mathbf{E}}=\sum_{n} \varsigma_n^+ \vec{\mathbf{E}}_n^+ + \sum_{\mathrm{n}} \varsigma_{\mathrm{n}}^- \vec{\mathbf{E}}_n^-,\ \vec{\mathbf{H}}=\sum_{n} \varsigma_n^+ \vec{\mathbf{H}}_n^+ + \sum_{\mathrm{n}} \varsigma_{\mathrm{n}}^- \vec{\mathbf{H}}_n^- \tag{1}$$

The complex amplitudes ($\varsigma_n^{\pm}$) may initially be undetermined, and the electromagnetic modal fields ($\vec{\mathbf{E}}_n^{\pm}$, $\vec{\mathbf{H}}_n^{\pm}$) must be known in advance (either analytically or numerically). This modal expansion provides a formal solution to Maxwell's equations, but in order to get a complete solution the boundary conditions must be satisfied at the interfaces between different regions.

In order to make computations easier, modal amplitudes from each region are usually organized into vectors which are related by the Generalized Scattering Matrix (GSM) [2][4]. The objective throughout the whole process would be to compute this GSM.

Although the modal expansion defines a complete representation of the electromagnetic field, in order to implement the Mode-Matching method on a real computer, the summations at (1) must be truncated, so convergence problems may arise. These problems will depend not only on the number of modes taken into account but also on the relation between the number of modes considered at each side of the discontinuity. This is known as the relative convergence problem.

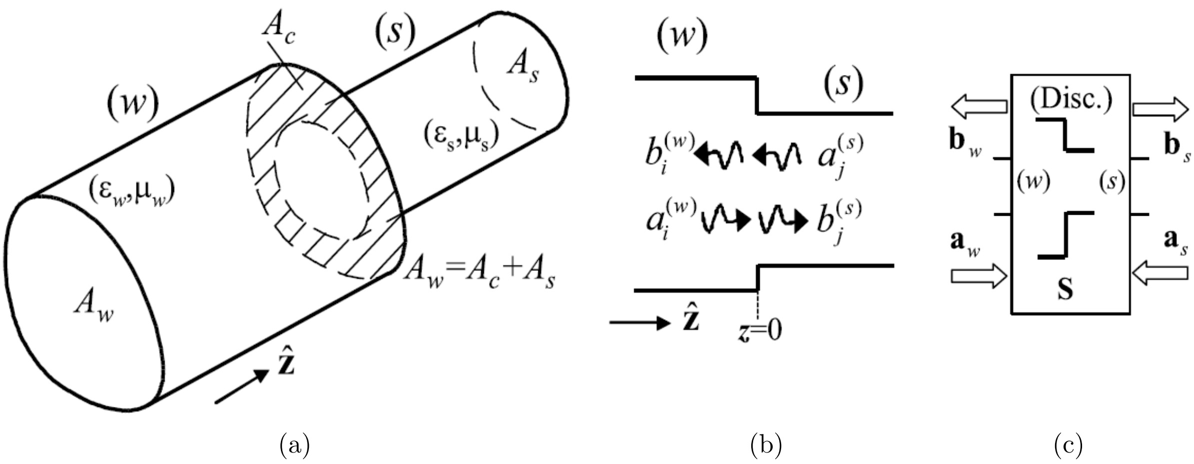

Figure 1: Single step representation [4]

In this paper the equations are only developed for the particular case where one section of the guide is completely included inside the other guide section ($A_s \subseteq A_w$, see Figure 1a). This simplification should not suppose a problem when dealing with most of the horn antennas. More complex cases can be analysed in a similar way [4].

Modal amplitudes at both sides of the discontinuity can be derived from the modal expansion. The boundary conditions must be fulfilled by the field component transverse to z evaluated at $z = 0^{\pm}$, according to Figure 1b. The transverse components of the fields at this point are expressed as a function of the incident and scattered modes.

$$\vec{\mathbf{E}}_t^{(w)}\Big\rfloor_{A_w,z=0^-} = \sum_{n=1}^{N_w}(a_n^{(w)} + b_n^{(w)})\vec{\mathbf{e}}_n^{(w)},\ \vec{\mathbf{H}}_t^{(w)}\Big\rfloor_{A_w,z=0^-} = \sum_{n=1}^{N_w}(a_n^{(w)} - b_n^{(w)})\vec{\mathbf{h}}_n^{(w)} \tag{2}$$

$$\vec{\mathbf{E}}_t^{(s)}\Big\rfloor_{A_s,z=0^+} = \sum_{m=1}^{N_s}(b_m^{(s)} + a_m^{(s)})\vec{\mathbf{e}}_m^{(s)},\ \vec{\mathbf{H}}_t^{(s)}\Big\rfloor_{A_s,z=0^+} = \sum_{m=1}^{N_s}(b_m^{(s)} - a_m^{(s)})\vec{\mathbf{h}}_m^{(s)} \tag{3}$$

Each term of the expansion corresponds with a TEM, TE or TM mode (not necessarily propagating at the operating frequency). It is also important to note that these modes are orthogonal with arbitrary normalization:

$$\iint_{A_g} \vec{\mathbf{e}}_n^{(g)} \times \vec{\mathbf{h}}_m^{(g)} \cdot \hat{\mathbf{z}} dS = Q_n^{(g)}\delta_{nm},\ g \equiv w, s,\ \delta_{nm} = \begin{cases} 1 & \text{if } m = n \\ 0 & \text{if } m \neq n \end{cases} \tag{4}$$

The boundary conditions at each interface between regions are:

$$\begin{cases} EFBC\, in\, A_w :\ \hat{\mathbf{z}} \times \vec{\mathbf{E}}^{(w)} = \begin{cases} 0 & in\, A_c, z = 0 \\ \hat{\mathbf{z}} \times \vec{\mathbf{E}}^{(s)} & in\, A_s, z = 0 \end{cases}, \\ MFBC\, in\, A_s :\ \hat{\mathbf{z}} \times \vec{\mathbf{H}}^{(w)} = \hat{\mathbf{z}} \times \vec{\mathbf{H}}^{(s)}\, in\, A_s, z = 0 \end{cases} \tag{5}$$

where EFBC stands for "Electric Field Boundary Conditions" and MFBC for "Magnetic Field Boundary Conditions". These conditions must be satisfied at both sides of the discontinuity.

The incident and scattered amplitudes (2), (3) are grouped in vectors. The normalization constants Q_n are grouped in a diagonal matrix and the following inner product is defined:

$$[X_{mn}] = \iint_{A_s} \vec{\mathbf{e}}_m^{(s)} \times \vec{\mathbf{h}}_n^{(w)} \cdot \hat{\mathbf{z}} dS \tag{6}$$

The following linear system [2][4] can be obtained from the boundary conditions:

$$\begin{cases} EFBC: & \mathbf{Q}_w(\mathbf{a}_w + \mathbf{b}_w) = \mathbf{X}^t(\mathbf{a}_s + \mathbf{b}_s)\, (N_w\, eqs.) \\ MFBC: & \mathbf{X}(\mathbf{a}_w - \mathbf{b}_w) = \mathbf{Q}_s(\mathbf{b}_s - \mathbf{a}_s)\, (N_s\, eqs.) \end{cases} \tag{7}$$

The GSM representation of the waveguide step relates the values of $\mathbf{b}_w$, $\mathbf{b}_s$(scattered waves) to the values of $\mathbf{a}_w$, $\mathbf{a}_s$(incident waves). This relation is expressed as:

$$\begin{bmatrix} \mathbf{b}_w \\ \mathbf{b}_s \end{bmatrix} = \begin{bmatrix} \mathbf{S}_{ww} & \mathbf{S}_{ws} \\ \mathbf{S}_{sw} & \mathbf{S}_{ss} \end{bmatrix} \begin{bmatrix} \mathbf{a}_w \\ \mathbf{a}_s \end{bmatrix},\ \mathbf{b} = \mathbf{S}\mathbf{a} \tag{8}$$

All the GSM sub-matrices can be obtained from (7):

$$\mathbf{S} = \begin{bmatrix} \mathbf{Q}_w^{-1}\mathbf{X}^t\mathbf{F}\mathbf{X} - \mathbf{I}_w & \mathbf{Q}_w^{-1}\mathbf{X}^t\mathbf{F}\mathbf{Q}_s \\ \mathbf{F}\mathbf{X} & \mathbf{F}\mathbf{Q}_s - \mathbf{I}_s \end{bmatrix},\ \mathbf{F} = 2(\mathbf{Q}_s + \mathbf{X}\mathbf{Q}_w^{-1}\mathbf{X}^t)^{-1}, \tag{9}$$

where $\mathbf{I}_g$ is the identity matrix of size N_g.

The procedure exposed above can also be used when working with complex structures made up of several waveguide discontinuities. The key idea is to divide the device under study in different steps, computing the GSM of each one of these steps and then computing the GSM of the whole structure by cascading the partial GSMs.

In order to illustrate this topic, the characterization of a waveguide with two discontinuities will be considered. Each of the steps can be pictured as a block (called block A and block B) whose GSM is known: $\mathbf{b}^{(A)} = \mathbf{S}^{(A)}\mathbf{a}^{(A)}$, $\mathbf{b}^{(B)} = \mathbf{S}^{(B)}\mathbf{a}^{(B)}$. These two blocks are connected by a waveguide of length l, where N_{AB} modes are considered. It is known that along this section of waveguide the modal amplitudes vary with $e^{-\gamma_n l}$ so the amplitudes at that region are related by:

$$\mathbf{a}_1^{(B)} = \mathbf{G}\mathbf{b}_2^{(A)},\ \mathbf{a}_2^{(A)} = \mathbf{G}\mathbf{b}_1^{(B)},\ \mathbf{G} = diag[e^{-\gamma l}]_{n=1,\ldots,N_{AB}} \tag{10}$$

And now compute:

$$\mathbf{S}^{(C)} = \begin{bmatrix} \mathbf{S}_{11}^{(A)} + \mathbf{S}_{12}^{(A)}\mathbf{G}\mathbf{H}\mathbf{S}_{11}^{(B)}\mathbf{G}\mathbf{S}_{21}^{(A)} & \mathbf{S}_{12}^{(A)}\mathbf{G}\mathbf{H}\mathbf{S}_{12}^{(B)} \\ \mathbf{S}_{21}^{(B)}\mathbf{G}(\mathbf{I}_{AB} + \mathbf{S}_{22}^{(A)}\mathbf{G}\mathbf{H}\mathbf{S}_{11}^{(B)}\mathbf{G})\mathbf{S}_{21}^{(A)} & \mathbf{S}_{22}^{(B)} + \mathbf{S}_{21}^{(B)}\mathbf{G}\mathbf{S}_{22}^{(A)}\mathbf{G}\mathbf{H}\mathbf{S}_{12}^{(B)} \end{bmatrix},$$
$$\mathbf{H} = (\mathbf{I}_{AB} - \mathbf{S}_{11}^{(B)}\mathbf{G}\mathbf{S}_{22}^{(A)}\mathbf{G})^{-1},\ [N_{AB}, N_{AB}] \tag{11}$$

This process is depicted in Figure 2 and by repeating it iteratively the GSM representing the whole device can be obtained.

3 MODELLING HORNS

3.1 Stage 1: Inside the horn

As stated before, the key idea of the method is to model the horn as a succession of waveguide steps and then to use a Mode-Matching software to simulate it. This process will provide the amplitudes of the modes at the aperture of the horn, which will be used in the next stage to compute the radiation pattern. The Mode-Matching software used in this implementation has been entirely developed by the authors of the paper.

The next problem that must be faced is the horn modelling. This task depends on the type of horn under study. This work only considers circular horns. In addition to the shape, horns can be classified as corrugated or smooth. Modelling corrugated horns is easy since by their own nature they are already "discrete". Each of the corrugations can be considered as a waveguide step.

The troubles appear when dealing with a non-corrugated horn. Two different methods have been implemented to accomplish the task of computing the discrete version of this type of antenna. They will be called the "hold" and the "middle-point" methods and a depiction of both can be found at Figure 3. Both methods divide the profile in sections of constant length. These sections will correspond with the waveguide sections of the

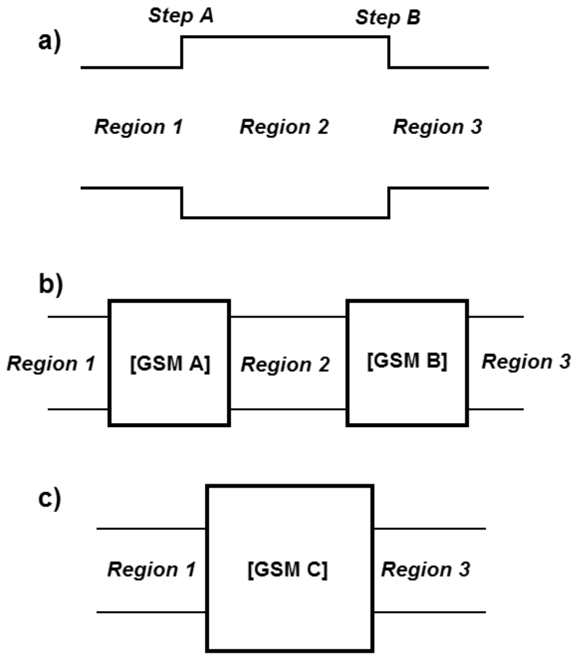

Figure 2: Cascading of two steps. a): Schematic representation of two steps. b): GSM of each step GSM. c): Cascaded GSM.

discrete model. The radius associated with each sections is computed differently by each discretization method. The "hold" method assumes that the waveguide section radius is equal to the radius of the horn at the the section end that is closest to the waveguide input. The "middle-point" method obtains the horn radius at both ends of the interval and then computes the waveguide section radius as the average of these two values.

It is important to note that convergence of the results must be studied by increasing the number of steps in which the horn is divided until it is noticed that the differences at the results become insignificant for the application under study. This convergence study must be also carried out for the number of modes used at the Mode-Matching simulation in equations (2), (3). Examples of these two types of convergence will be seen in next section.

3.2 Stage 2: Outside the horn

The previous step provides with an array of coefficients representing the amplitudes of the modes at the horn aperture. These modes can be used to compute the radiation pattern for the antenna under study. First of all, the total electric field at the horn aperture has to be obtained. It can be obtained as:

$$\vec{\mathbf{E}}_{ap} = \begin{cases} \sum_m \left\{ A_m^{TE} \vec{\mathbf{e}}_m^{TE} + A_m^{TM} \vec{\mathbf{e}}_m^{TM} \right\} & 0 \le r \le a \\ 0 & otherwise \end{cases}, \tag{12}$$

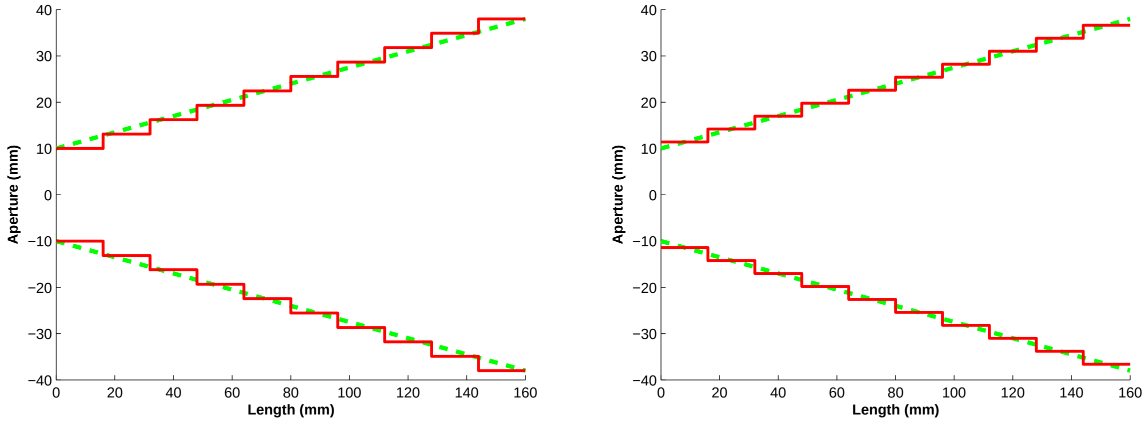

(a) Hold method.

(b) Middle point method.

Figure 3: Discretization methods of the horn profile.

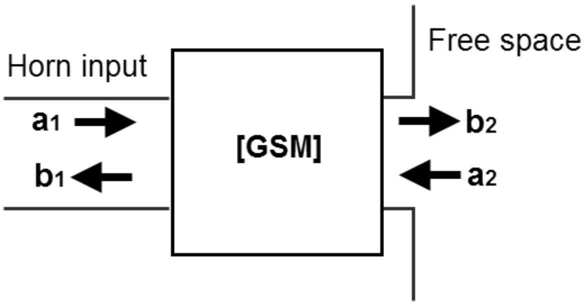

Figure 4: Horn antenna characterized by its GSM.

where a is the horn aperture radius and A_m^{TE}, A_m^{TM} and $\vec{\mathbf{e}}_m^{TE}, \vec{\mathbf{e}}_m^{TM}$ are the amplitudes (referred as b_2 in Figure 4) and the modes scattered at a discontinuity as expressed in (2) and (3) respectively. The TE modes have been separated from the TM to simplify notation in the following integrations[1]. To obtain the radiated field at the far-field region the transverse field must be integrated at the aperture [3]:

$$\vec{\mathbf{E}} = \frac{jke^{-jkr}}{4\pi r}(1+\cos(\theta))a\int_0^1\int_0^{2\pi}\vec{\mathbf{E}}_{ap}e^{jkar\sin(\theta)\cos(\phi-\phi')}rdrd\varphi \qquad (13)$$

The calculation of this integral is found in [3]:

[1]For the problem under study only the TE_{c1r} and TM_{s1r} modes are used. These are the only modes that have to be considered if the horn is excited only with the fundamental mode at the input waveguide and the horn presents revolution symmetry. Its field expressions can be found in [5]

$$E_\theta = \frac{ke^{-jkr}}{2r}(1+\cos(\theta))a^2\sin(\phi)\sum_m [A_m^{TE}K_m^{TE} jJ_1(p'_{1m})\frac{J_1(ka\sin(\theta))}{ka\sin(\theta)} - \\ - A_m^{TM}K_m^{TM} jp_{1m}J'_1(p_{1m})\frac{kaJ_1(ka\sin(\theta))}{(p_{1m})^2-(ka\sin(\theta))^2}] \quad (14)$$

$$E_\phi = \frac{ke^{-jkr}}{2r}(1+\cos(\theta))a^2\cos(\phi)\sum_m [A_m^{TE}K_m^{TE}(p'_{1m})^2 J_1(p'_{1m})\frac{J'_1(ka\sin(\theta))}{(p'_{1m})^2-(ka\sin(\theta))^2}] \quad (15)$$

The radiation intensity [1] can be computed as:

$$U = \frac{r^2}{2\eta}\left[|E_\theta|^2 + |E_\phi|^2\right] \quad (16)$$

And the directivity [1] as:

$$D = \frac{4\pi U_{Max}}{P_{rad}} \quad (17)$$

Where P_{rad} can be obtained from the GSM as[2]:

$$P_{rad} = 1 - |S_{11}^{GSM}|^2. \quad (18)$$

This last equation assumes that the horn is lossless.

4 VERIFICATION CASES

After developing the simulation software it is important to check whether the implementation is working correctly. To perform this verification a set of horns are simulated and the results obtained with the Mode-Matching software are compared with data obtained by other authors.

4.1 "Tercius" test antenna

As a first example a simple horn antenna is considered, which has been called "Tercius". This device is just a concatenation of some waveguide steps and although its radiation pattern is not really useful to be used in a real case, the structure is simple enough to be simulated using a commercial tool as CST Microwave Studio. The dimensions of each waveguide section can be found at Table 1.

Direct simulation of this antenna with CST took approximately two orders of magnitude in time more than with the mode-matching code. Although this is just a particular

[2]If the modes have been normalized and $Q = I$ then P_{rad} should also be divided by 2. Note that in the Poynting theorem there is a factor of two dividing the surface integral.

Radius (mm)	Length (mm)
5	10
10	10
15	10
20	10
25	10
30	10
35	10
40	10
45	10
50	10

Table 1: Dimensions of the waveguide steps (10 waveguide sections) at "Tercius" test antenna.

performance test, the comparison should at least give some insight of the advantages obtained by using mode-matching rather than generic numerical methods, when the structure under analysis is suitable for a mode-matching analysis. The number of modes considered at the input waveguide and at the aperture were 7 and 70, respectively.

The results of the radiation pattern are depicted in Figure 5 superimposed onto the radiation pattern obtained with CST. It can be seen that the results for the main lobe are almost identical and they start to diverge at the first side lobe. Since horn antennas are very directive these should not be an issue for more practical cases.

4.2 High Performance Feed Horn

The next verification case is a smooth horn with three sections of different slope. The profile of this horn can be divided into three regions of smooth continuous shape. The discretization process described in section 3 has been applied to each of these sections and then the three discrete models have been be put together in order to get a model of the whole antenna. The profile can be found at Figure 6.

This antenna was designed, constructed and measured by [6]. The results obtained by the Mode-Matching software have been compared with the measurements by the original authors using graphical superposition. The computed radiation pattern at $700GHz$ can be seen at Figure 7, with very good agreement.

4.3 Convergence

All the verification cases have been presented in previous figures showing the final results, postponing the convergence study associated to the used numerical method to this section. The different sources of problems that have to be taken into account for this numerical method are analysed now.

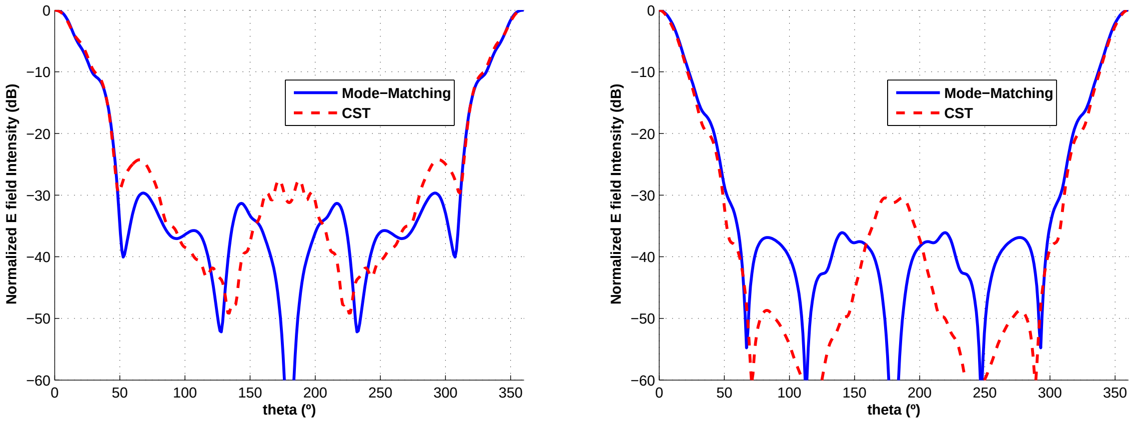

(a) E-Plane($\phi = 90°$). $D_{0,MM} = 16.58dBi$. (b) H-Plane($\phi = 0°$). $D_{0,MM} = 16.58dBi$.

Figure 5: “Tercius” test antenna radiation pattern. Comparison between Mode-Matching computation and CST Microwave Studio.

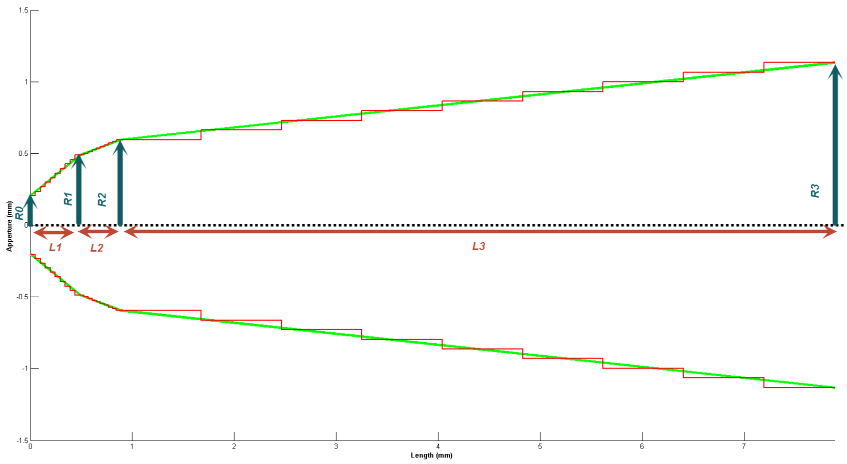

Figure 6: Profile of the High Performance Feed Horn. Dimensions R0, R1, R2, R3, L1, L2 and L3 have been extracted from [6]. Red stairs represent the discrete version of the horn. A low number of steps has been used so they are easily visible.

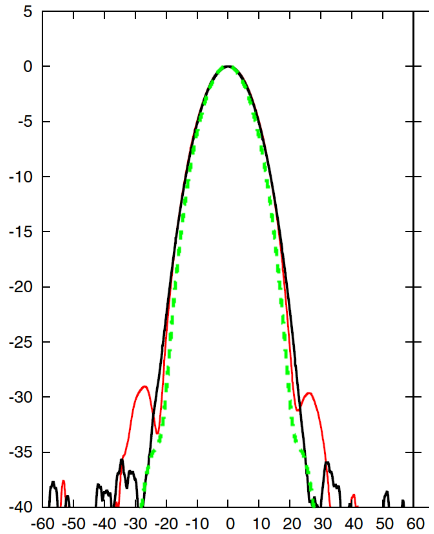

(a) E-plane ($\phi = 90°$). Solid red: Measurements. Dashed green: Mode-Matching.

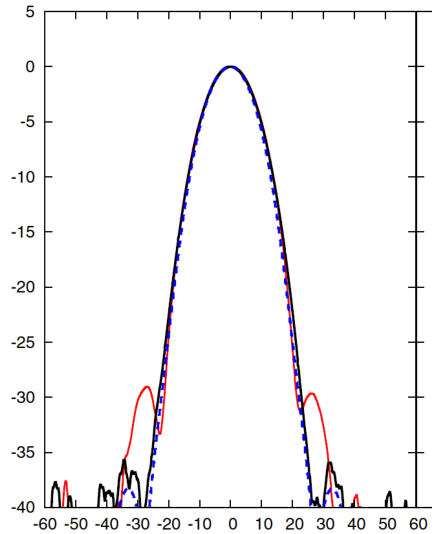

(b) H-Plane ($\phi = 0°$). Solid red: Measures. Dashed blue: Mode-Matching.

Figure 7: High performance feed horn simulation compared with measurement data by [6].

In the developed software convergence problems may arise from three different factors: the discretization method used to model the horn, the number of waveguide steps used in this discretization and the number of modes considered when performing the Mode-Matching analysis.

In this convergence analysis the conical horn presented by [7] will be analysed under different simulation conditions. The conclusions obtained for this analysis could be also extended to other cases.

Figures 8 and 11 demonstrate, as stated before, that the discretization method used does not practically affect the results. The number of modes at the aperture was 70 and the number of steps while discretizing were 100 (for the radiation pattern) and 160 (for the return losses).

As it is shown by Figures 9 and 11, it is not necessary to use a large number of modes to achieve convergence. As it can be seen, increasing the number of modes gives a more accurate computation of the side lobes but does not change significantly the main lobe. This contributes to make the computations faster. The discretization method used at this test was the “middle-point” with 100 steps for the radiation pattern and 160 steps for the return loses. It is important to note that the number of modes expressed at the figure legend refers to the modes at the aperture of the antenna. The number of modes at each waveguide step must be computed accordingly at the radius of the discontinuity.

The convergence analysis reveals that the most influential parameter is the resolution used to create the discrete model. As it can be seen in Figures 10 and 11, low values

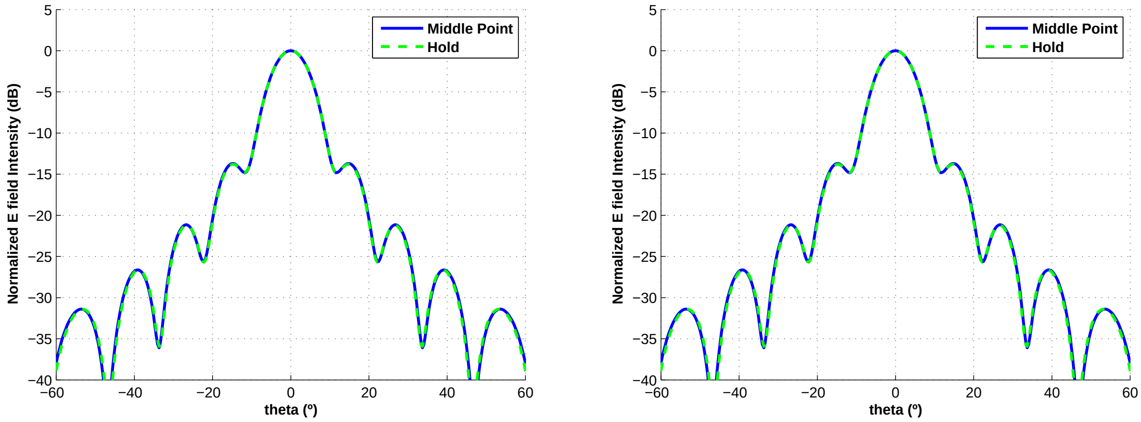

(a) E-plane ($\phi = 90°$).

(b) H-Plane ($\phi = 0°$).

Figure 8: Convergence of the radiation pattern for different discretization methods.

of this parameter give non satisfactory results not only at the side lobes but also at the main lobe. Convergence occurs for values around 100 steps. Indeed, a bad setting of this parameter can have a great impact not only on the convergence of the radiation pattern but also on the computation of the return loss. The chosen discretization method was the "middle-point" and the number of modes at the aperture was 70.

5 CONCLUSIONS

The main goal of this work has been to develop a method for analysis and design of horn antennas that would give shorter computation times than the commercial tools. Using the Mode-Matching method, a code capable of modelling a horn antenna has been developed.

After the implementation step the validity of the software has been verified in two different ways. First, the computed parameters were compared against data from other sources (different numerical methods, measurements by other authors...) and after that, the converge of the method has been studied.

Once the software is completely verified, it can be incorporated to the antenna design process. This tool may replace the commercial (and resource demanding) CAD tools at the first stages of the design, when several simulations are required in order to optimize the design parameters of the device. Using the Mode-Matching software implemented in this work would allow to significantly reduce the computation time when performing parametric sweep simulations. When a satisfying design is achieved a commercial tool like CST Microwave Studio or any other full-wave software may be used as a verification step before constructing the antenna, or to include other effects not considered in the initial simulations.

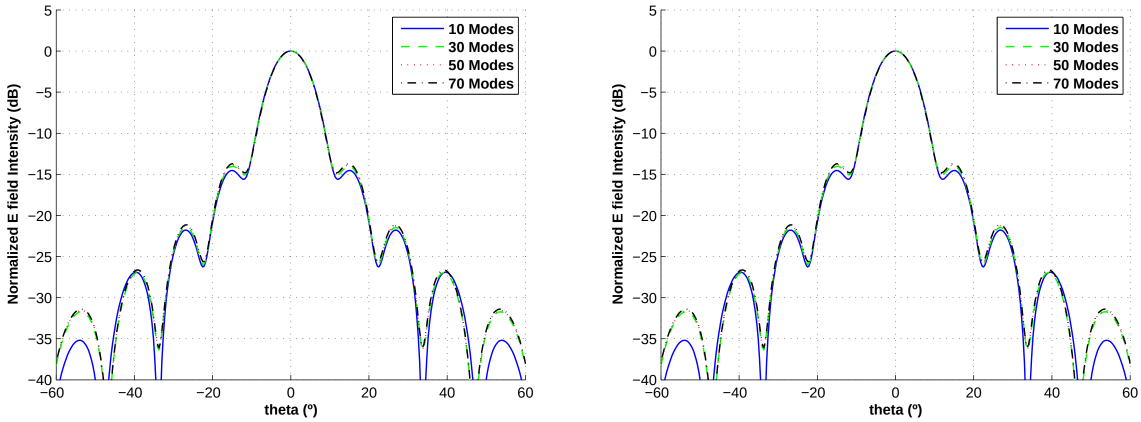

(a) E-plane ($\phi = 90°$).

(b) H-Plane ($\phi = 0°$).

Figure 9: Convergence of the radiation pattern for different number of modes at the horn aperture.

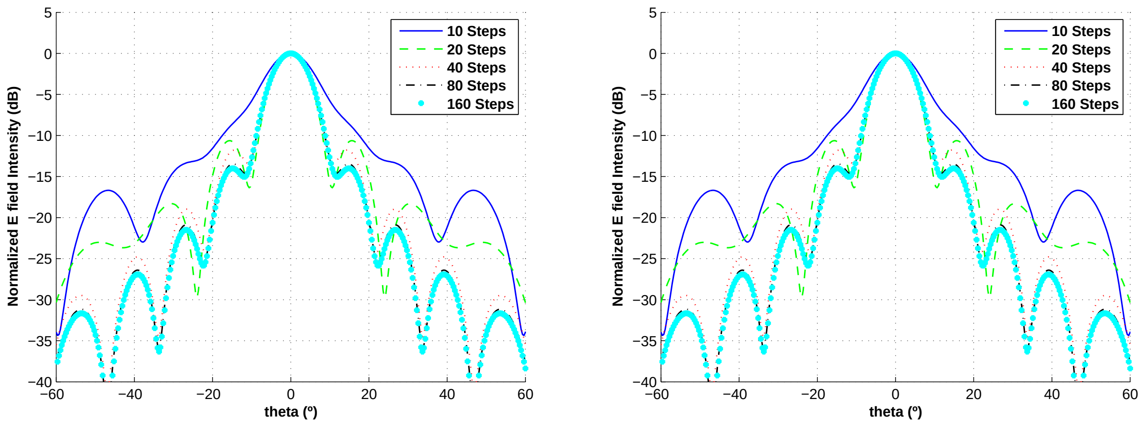

(a) E-plane ($\phi = 90°$).

(b) H-Plane ($\phi = 0°$).

Figure 10: Convergence of the radiation pattern for different number of waveguide steps.

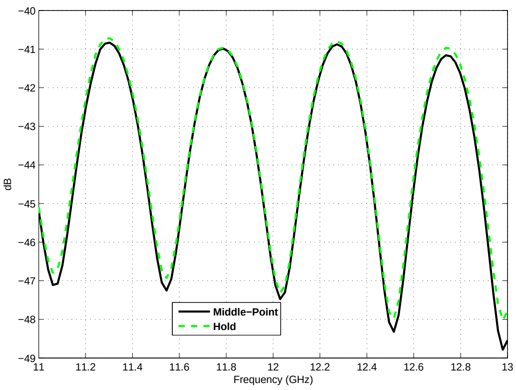

(a) For different discretization methods.

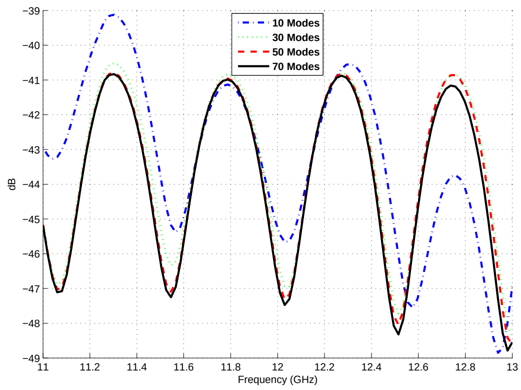

(b) For different number of modes.

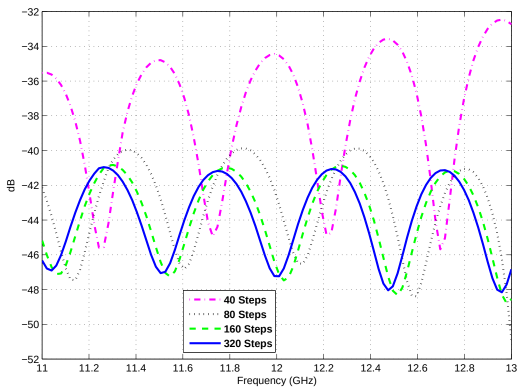

(c) For different number of waveguide steps.

Figure 11: Convergence study of the return losses.

Due to the high efficiency achieved by the Mode-Matching method, the software can be easily combined with an optimization algorithm like gradient descent in order to carry out an automatized optimization of the design parameters (for example, beamwidth versus aperture diameter). Doing this kind of task using general purpose commercial tools usually leads to large computation times while using a Mode-Matching implementation may take just some minutes.

REFERENCES

[1] Balanis C. A. "Antenna Theory, Analysis and Design", Third Edition. John Wiley & Sons, 2005.

[2] A. Wexler, "Solution of waveguides discontinuities by modal analysis", IEEE Transactions on Microwave Theory and Techniques, vol. 15, pp. 508 - 517, sep 1967.

[3] A. Ludwig, "Radiation pattern synthesis for circular aperture horn antennas", Antennas and Propagation, IEEE Transactions on, vol. 14, no. 4, pp. 434 - 440, Jul. 1966.

[4] Ruiz-Cruz, J.A. Montejo-Garai, J.R. Rebollar, J.M. "Computer Aided Design of Waveguide Devices by Mode-Matching Methods" in "Passive Microwave Components and Antennas" Published by In-Teh, 2010. ISBN 978-953-307-083-4

[5] Pozar, D.M. "Microwave Engineering", Fourth Edition. John Wiley & Sons, 2012

[6] Tan, Boon-Kok. Leech, Jamie. Yassin, Ghassan. Kittara, Phichet. Tacon, Mike. Wangsuya, Sujint. Groppi, Christopher. "A High Performance 700 GHz Feed Horn", in Journal of Infrared, Millimeter, and Terahertz Waves, 2012. Springer US, vol. 33, issue 1, pp.1-5.

[7] J. Reiter and F. Arndt, "Full-wave analysis of circular waveguide horn antennas including the outer wall geometry with an hybrid MM/BCMM method", in "Antennas and Propagation Society International Symposium, 1996". AP-S. Digest, vol. 3, pp. 1984-1987, Jul 1996.